Applied Radiation and Isotopes 208 (2024) 111302

Contents lists available at ScienceDirect

Applied Radiation and Isotopes

journal homepage: www.elsevier.com/locate/apradiso

Thermal neutron dose measurements using TLD-100 detectors in the IPEN/MB-01 reactor core

Tássio Antonio Cavalieri, Paulo de Tarso Dalledone Siqueira *, Julian Marco Barbosa Shorto, Helio Yoriyaz

Instituto de Pesquisas Energéticas e Nucleares, IPEN-CNEN, Brazil

ARTICLE INFO

Keywords:
Mixed radiation fields
Monte Carlo
Research reactor
TLD-100

ABSTRACT

Considerable experimental effort has been aimed at uncovering a reliable way to perform a dosimetric assessment in mixed radiation fields. In fields composed by gammas and neutrons, TLD dosimeters are usually applied to execute such measurements, although there is no consensus on the most favorable strategy to employ them. In this context, TLD-100 measurements within two different core configurations of the IPEN/MB-01 research reactor and Monte Carlo simulations have been used to investigate the behavior of those detectors in multiple mixed radiation fields, deriving a methodology to evaluate the dose deposition in the dosimeter by different gamma and neutron energy spectra and intensities. A surprising outcome is the linear neutron dose response shown by TLD-100 even irradiated by so distinct irradiation fields.

1. Introduction

It is well known that patients who undergo Neutron Capture Therapy (NCT) are exposed to a complex irradiation field composed by different radiation components, including neutrons and gammas (Gambarini et al., 2015a). In proton therapy (PT) a cascade of particles is generated from the interaction with the medium forming a mixed radiation field (Lee et al., 2015). Even in conventional radiotherapy using megavoltage photon beams the production of photoneutrons should be considered to correctly estimate dose (Hakimi and Sohrabi, 2017).

Thermoluminescent dosimeters (TLDs) are among the commonly applied tools for dose measurements in mixed radiation field. More specifically, some groups have been studying different kinds of TLDs in the high neutron flux environment usually found in nuclear reactors. Gambarini et al. (2015b) measured the gamma component in the LVR-15 reactor at the Research Center Rez at 9 MW operating power, producing epithermal and thermal neutron fluxes of 6.5×10^8 cm^{-2} s^{-1} and 3.8×10^7 cm^{-2} s^{-1}, respectively. They analyzed in mice phantom the suitability of TLD-600 and TLD-700 glow curve (GC) peak responses and Frick gel dosimeters to determine spatial distribution of doses due to gamma and to the (n, ^{10}B) reaction. Ekendahl et al. (2018) studied the neutron sensitivity of common salt (NaCl) in a mixed radiation field and found it comparable with neutron sensitivity of TLD-700. They irradiated the salt detector in the VR-1 reactor at the Czech Technical University with an assumed total neutron flux of 5.55×10^8 cm^{-2} s^{-1}. Gamma dose was measured using optically stimulated luminescence (OSL) technique, although it could be overestimated due to NaCl self-irradiation. Torkzadeh and Manouchehri (2006) successfully utilized TLD-600 for thermal neutron fluence measurement at the Tehran Research reactor in the range of 10^{11} to 10^{13} n.cm^{-2} varying the reactor power and the irradiation time. Differences between TL responses from bare and Cd-covered TLDs were estimated to obtain the thermal neutron fluence. Tsai et al. (2018) used TLD-400 (CaF2:Mn) to measure the gamma dose component in a PMMA phantom exposed to a BNCT beam generated in the Tsing Hua Open-pool 2 MW Reactor (THOR). As this type of dosimeter presents very low neutron sensitivity, the neutron contribution to the TL signal was less than 0.3%. Measurement uncertainty was reduced as each TLD-400 chip was considered a single detector with his own calibration factor, and the gamma component was adequately determined.

To contribute to the current knowledge of dose measurements in mixed radiation field, we investigated whether TLD-100 presents specific dose response calibration curves according to a determined mixed radiation field or preserves a unique dose response function regardless of the radiation field. Therefore TLD-100 has been irradiated at different mixed fields presenting changes in neutron energy spectra, neutron gamma relative contributions, and total field intensities. To carry out the experiments TLD-100 dosimeters were irradiated in the IPEN/MB-01

* Corresponding author.
E-mail address: ptsiquei@ipen.br (P.T. Dalledone Siqueira).

https://doi.org/10.1016/j.apradiso.2024.111302
Received 3 April 2019; Received in revised form 24 May 2023; Accepted 19 March 2024
Available online 24 March 2024

research reactor at the Nuclear and Energy Research Institute, IPEN-CNEN (Brazil) (dos Santos et al., 2013; van der Marck, 2012; Zoia et al., 2017).

This reactor presents a construction flexibility that permits to be operated at different reactor core configurations as well as the introduction of TLD sets in its core at controlled reactor power and moderator temperature. A great sort of mixed neutron-gamma radiation fields has been driven along the reactor core to perform dosimetric studies. In this sense, TLD-100 sets were exposed to irradiation fields presenting great differences on neutron energy spectra and neutron/gamma balance and intensities. TLD Experimental results have been associated to the calculated irradiation parameters as the reactor benchmarked design quality allows to calculate with MCNP the radiation field components with great confidence and to discriminate between neutron and gamma doses delivered to the dosimeters.

2. Materials

2.1. TLD dosimeters

Thermo Scientific™ LiF:Mg, Ti thermoluminescent dosimeters, TLD-100, in the format of disk with 3 mm of diameter and 0.38 mm of thickness were used through the work. This dosimeter presents the natural isotope abundance of Li (7.5% of ^{6}Li and 92.5% ^{7}Li). Two other LiF dosimeters are often used: TLD-600 and TLD-700. They distinguish from each other and from TLD-100 by ^{6}Li and ^{7}Li abundances. TLD-600 is ^{6}Li; enriched while TLD-700 is ^{6}Li depleted. As ^{6}Li presents high cross section for thermal neutrons, TLD-600 is frequently used to estimate the neutron dose, i.e. the dose component delivered by neutrons, while TLD-700, with minimal amount of 6Li is used to estimate the gamma dose.

Fig. 1 presents TLD 100 glow curves for two distinct field expositions: a mixed neutron gamma field, such one of the fields evaluated in this work, and a pure gamma field, such as the ^{60}Co field used to select the dosimeters. The TL curve registers the amount of light emitted by the TLD as its temperature is raised. LiF TLDs glow curve presents two main region of interest (ROIs) formed by several peaks. The first region of interest (ROI 1) corresponds to the light emission region around 195 °C and encompasses the main LiF dosimetric peaks. ROI 1 is commonly used in TL dosimetry as it comprises the TL peaks with most intense responses to gamma radiation and which are less susceptible to fading (Pradhan, 1981). The second region of interest (ROI 2) corresponds to the light emission region around 250 °C and is particularly sensitive to neutrons (Triolo et al., 2007; Carrillo et al., 1987), as it contains the peaks which are mainly expressed by the TLD interactions with neutrons.

The TLD measurement process was performed in a three-day cycle: TLD annealing in the first day; irradiation in the second day; and TLD reading in the third day. The annealing procedure followed the manufacturer recommendations, i.e., the TLDs are annealed at 400 °C for 1 h and at 100 °C by 2 h afterward. The TLDs were read using a Harshaw TLD 3500 reader. The reading cycle consisted in a linear warming up with a 10 °C/s rate, data acquisition starting at 60 °C and ending at 400 °C, in a total region of 200 channels. The glow curve was acquired during a period of time of 45s, with the temperature resting at 400 °C in the last 11s.

2.2. IPEN/MB-01 research reactor

The IPEN/MB-01 reactor is a nuclear research reactor primarily used as an experimental benchmark. It was conceived to provide a large experimental flexibility, thus it has been operated at a broad variety of core configurations, having both experimental and simulated neutron flux well determined (Bitelli et al., 2009, dos Santos et al., 2012). By the time our experiments were carried out the reactor core consisted basically of a set of fuel rods which are distributed along a 30 × 30 rectangular matrix (bottom grid plate). Two banks of control rods (Ag–In–Cd) and two banks of safety rods (B_4C) were displaced in distinct quadrants of the core completing the basic reactor core components. The fuel rods were essentially made of the nuclear fuel UO2 pellets (enriched at 4.3% in weight) which were piled together along 54.6 cm the stainless steel (SS-304) cladding tube. The fuel length along the vertical axis is known as the active core height. The fuel rod external diameter was 0.98 cm and the lattice pitch, i.e. the distance between the center of neighboring elements, was 1.5 cm. The core was settled inside a 200 cm height by 200 cm diameter cylindrical water tank. The reactor may be run up to a maximum allowed 100 W power.

2.3. MCNP5 code

Flux and dose distributions due to different field components at different locations inside the reactor core have been calculated using the radiation transport code MCNP5 (X-5 Monte Carlo Team, 2003). For this purpose, we simulated the entire reactor core for both configurations and the calculated fluxes were validated with experimental data given by previous works (Bitelli et al., 2007; Gonçalves, 2008).

Neutron and gamma fluxes were calculated by the MCNP track-length estimator (tally F4). This tally considers the statistical weight W and energy E of the particle and calculates the track-length (segment) T within a specified cell of volume V. This segment makes a contribution of WT/V to the fluence in the cell. The sum of the contributions is reported as the F4 tally in the MCNP output in units of particles.cm^{-2}. This is equivalent to the fluence calculation according to equation (1), where $\varphi_x(\vec{r}, E, \vec{\Omega})$ is the energy and angular distribution of particles ($x = p$, for photons or $x = n$ for neutrons) as a function of position (Shultis and Faw, 2011). Neutron flux was calculated for three energy ranges: thermal neutrons (En $\leq$ 0.625 eV); epithermal neutrons (0.625 eV $<$ En $\leq$ 100 keV); and fast neutrons (En $>$ 100 keV).

$$F4 = \frac{1}{V}\int dV \int dE \int d\vec{\Omega}.\varphi_x\left(\vec{r}, E, \vec{\Omega}\right) \quad (1)$$

Gamma doses in the TLDs were calculated modifying equation (1) and introducing the mass energy-absorption coefficient, $\mu_{en}/\rho(E)$, of the material, which is provided to the MCNP code by using the DE/DF cards (see equation (2) below). In this work, it was used the mass energy-absorption coefficient of TLD-100 (LiF) obtained from NIST (NIST, 2010).

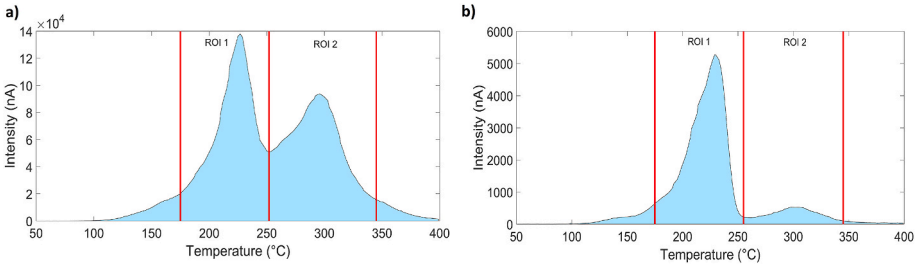

Fig. 1. LiF TLD-100 Regions of Interest, 1 and 2, after an exposition to: a) mixed neutron gamma field; b) gamma field.

$$D^{gamma} = \frac{1}{V}\int dV \int dE.E.\frac{\mu_{en}}{\rho}(E) \int d\overrightarrow{\Omega}.\varphi_p\left(\overrightarrow{r},E,\overrightarrow{\Omega}\right) \quad (2)$$

The neutron dose was calculated using the tally F4 with the FM card. FM allows coupling neutron flux with a variety of energy dependent functions such as material cross sections. This card was used to modify neutron flux estimates, driven from tally F4, into dose estimates. Therefore neutron fluxes tallies were multiplied by material total cross section ($\sigma_t(E)$) and by the average reaction heating number ($H(E)$) according to equation (3). The ρ_a/m coefficient at the beginning of equation is the atom density (atoms.barn^{-1}.cm^{-1}) per unit of target mass (g) ratio which accounts for setting the results into the MeV.g^{-1} dose unit.

The cross-section libraries used at simulations were: ENDF/B.VI.6 for neutrons; MCPLIB-04 for gamma transport; and lwtr.10t for thermal neutron scattering in water.

$$D^{neutron} = \frac{\rho_a}{m}.\int dE \int dV \int d\overrightarrow{\Omega}.\sigma_t(E).H(E).\varphi_n\left(\overrightarrow{r},E,\overrightarrow{\Omega}\right) \quad (3)$$

3. Experimental design and methodology

As said before, IPEN/MB-01 provides a great variety of mixed radiation fields and its radiation field parameters may be estimated by simulation with great confidence. Therefore, simulations have been run to identify specific spots within different core configurations where radiation fields might present distinct formats or intensities.

Two core configurations were drawn from simulations (Fig. 2): one to investigate the TLD-100 response under different fields and a second one as an experimental validation configuration to check the maintenance of the dose response curve even when applied to different core and radiation field configurations. Fig. 2a shows a schematic view of the cylindrical core configuration, used in the investigative TLD irradiations, while Fig. 2b shows the rectangular 26 × 28 fuel rod core configuration, used in experimental validation. The core configurations differ not only by the fuel rod distribution but also by the number of fuel rods used. Fuel rods were also removed from the center of the cylindrical core configuration, so to leave space for water, the moderator material of the reactor. This water region increases the thermal neutron flux and is therefore known as a neutron flux trap.

For each core configuration, 12 locations presenting both distinct radiation field formats and intensities have been selected for TLD positioning. These places were arranged in a 2 × 3 x 2 matrix disposition: two core channels (central and peripheral, as illustrated in Fig. 2) and three positions (0, 9 and 18 cm) along two parallel lines with different heights (27.3 and 45.6 cm), as shown in Fig. 3.

Once the locations and configurations worth investigating have been determined, a set of TLD-100 irradiations was devised to exploit those mixed fields with different compositions.

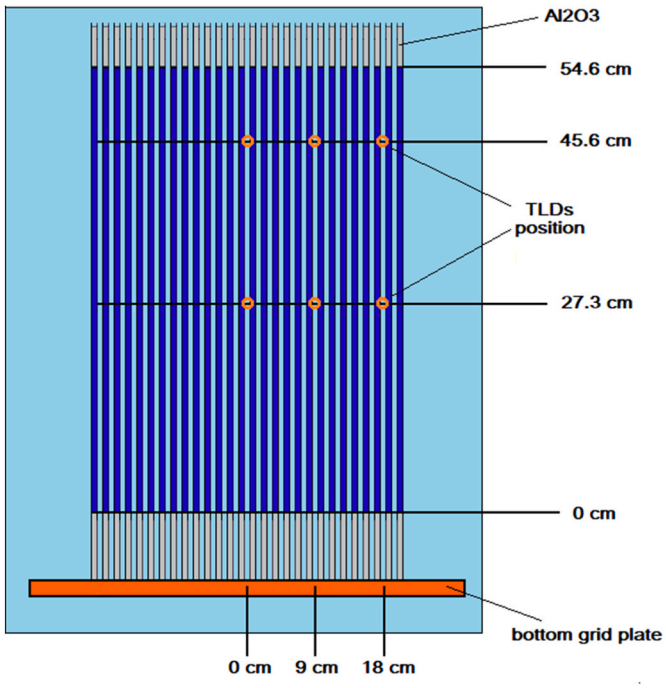

Fig. 3. Schematic vertical view of the TLD positions in the reactor core (rectangular configuration).

3.1. Irradiations

To conduct the TLD irradiations, sets of 3 TLDs packed with a thin plastic film have been assembled. Thereafter, these packs were placed at 6 positions on a 7 mm thick PMMA support plate, in a 3 × 2 matrix disposition, covering the 6 locations highlighted in Fig. 3. Several benchmarks experiments performed previously demonstrated that the PMMA support plays no impact on the measurements. Prior to reactor operation, this PMMA plate was positioned within the reactor core along one of the 2 selected channels described before. Each reactor operation lasted for one hour at a 1 W thermal power. This operation setup was chosen to enable the removal of the TLDs shortly after reactor shutdown and thus reducing the time that TLDs would be exposed to residual radiation. A total of four irradiations were done, as the TLDs were irradiated along the central and peripheral channels for both cylindrical and rectangular core configurations.

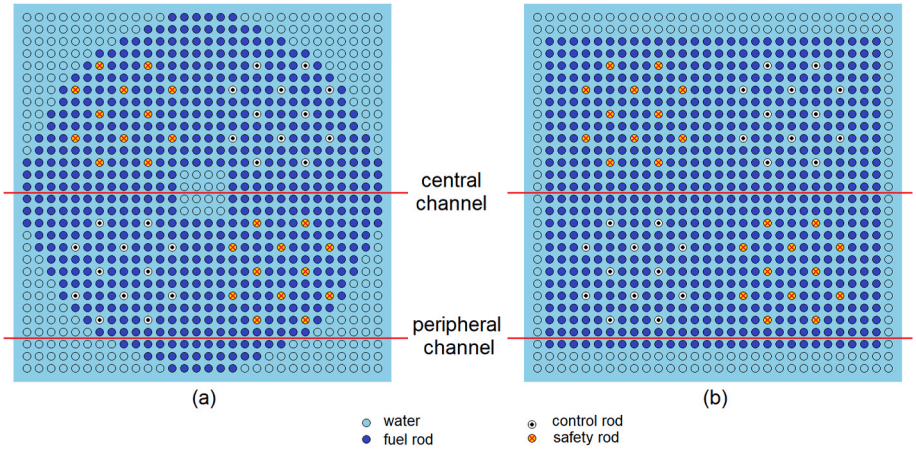

Fig. 2. Horizontal views of the configurations of the IPEN/MB-01 reactor core: a) cylindrical with flux trap; b) rectangular.

4. Results and discussion

Simulated fluxes and doses and experimental TLD responses were obtained for each of the selected irradiation spots for both core configurations: cylindrical to investigate the field variation effect on TLD-100 response; and rectangular as experimental validation test.

Simulations and experimental results for the cylindrical configuration are shown together, providing a qualitative link between TLD responses and radiation field variations. In addition, a quantitative analysis indicating the correspondence between TLD-100 response and neutron dose is also presented.

These presentations were limited to one configuration quota (z = 27.3 cm), i.e. to half of the existing simulated and experimental data, as differences between the 2 distinct quotas are only observed in their intensities, they preserving the same qualitative behavior.

At last, to evaluate the experimental methodology, it is exhibited a comparison of neutron doses calculated by two distinct approaches, Monte Carlo simulations and the proposed correspondence to TLD-100 response.

4.1. Investigative TLD irradiations

Fig. 4 presents simulated photon and neutron (fast, epithermal and thermal) flux profiles at 27.3 cm height along the central channel of the cylindrical configuration with a maximum statistical uncertainty of 1%. Simulated irradiation conditions are the same as described in section 3.1. TLD-100 responses of ROIs 1 and 2 measured at positions 0, 9 and 18 cm are also shown in Fig. 4 in a superposed way, with the scale axis laying at the right of the figure. Each plotted value corresponds to the average of three TLD responses. Experimental uncertainties due to TLD positioning imprecision and TLD reading fluctuations are estimated as being 10% of the average values.

Clear differences between flux profiles of the field components shown in Fig. 4 can be observed. The photon flux profile (magenta line) presents a flat plateau around its maximum value at the center of the core along the entire flux trap region. Photon flux also decreases almost linearly as it departs from the center to the core outer limits. Neutron flux profiles show different patterns: while the epithermal neutron flux profile (yellow line) follows a similar trend to that of the photon flux profile with a lower magnitude; thermal and fast neutron flux profiles (blue and green lines, respectively) show a clear interplay between them. This correlation is clearly indicated by the inversions of the main neutron energy component along the channel. Thermal neutrons prevail at the center of the reactor core, which is a moderator rich region due to the flux trap. Fast neutrons, on the other hand, prevail in the core at the active area zone, where the fission material lies. A slight oscillation on thermal neutron flux profile can be observed at the active area zone due to the narrowing of the water channel between fuel rods.

As pointed out in section 3, radiation composition profile changes greatly along the central channel of the cylindrical configuration, and TLD positioning was designed to seize this change. Although TLD responses (right axis) and calculated flux profiles (left axis) are plotted at different scales, both ROIs 1 and 2 seem to follow the thermal neutron flux variations, as they present similar radial profile, i.e. a huge response drop between the central and intermediate positions and a mild response decrease between intermediate and external positions.

Fig. 5 shows the calculated neutron dose which would be delivered to the TLD-100 if it had been submitted to the radiation field shown in the previous figure. As calculated gamma dose values are at least 40 times less than calculated neutron dose values, they were not shown in the figure. TLD-100 experimental data are presented once more for comparison.

The maximum neutron and photon doses occur at the center of the flux trap and are respectively 58 ± 2 Gy and 1.74 ± 0.03 Gy.

A qualitative comparison of Figs. 4 and 5 seems to indicate that in these irradiation conditions the delivered dose to TLD-100 is insensitive to neutron components other than the thermal. The high ^{6}Li (n,α) cross section and its associated energy release account for most of the energy delivered to TLD-100 despite ^{6}Li low isotopic abundance. This effect is not restricted to ROI-2 as it would be expected, but also extended to ROI-1, usually associated to both gamma and neutron energy delivering process. This is consequence of the reduced gamma contribution to the dose imparted to TLD-100 when compared to the neutron contribution.

Figs. 6 and 7 are analogous to Figs. 4 and 5, but they bring information concerning the peripheral channel. Except for this channel swap, all remaining experimental and calculation details stay the same.

Once again, one can observe the clear differences along the flux profiles of the radiation field components shown in Fig. 6. Gamma, fast neutron and epithermal neutron fluxes have their maximum value at the center of the peripheral channel. However, the fast neutron flux profile presents a more accentuated flux decrease than do the gamma flux as one leaves the active volume of the core. Thermal neutron flux on its turn has its maximum value out of the active volume, i.e. at the reflector domain. Its value, except for the fluctuations due to changes on the moderator thickness along the channel, which has been observed in Fig. 4 as well, barely changes along the reactor core active volume.

Fig. 7, which depicts simulated neutron dose deposited to the TLD, confirms what is observed before in Fig. 5: in these irradiation conditions, thermal neutrons are the mainly contributors to the delivered dose on TLD-100.

TLD-100 responses are once again plotted over the calculated flux and dose profiles (left axis) but at a different scale (right axis). As occurred before in the central channel, the TLDs were able to catch the radiation composition changes along the peripheral channel, and ROIs 1 and 2 also seem to follow the thermal neutron flux profile, showing a clear response increment for the outermost position showing the same response profile of the thermal neutron component.

Table 1 presents the calculated fluxes and doses ratios at all spots

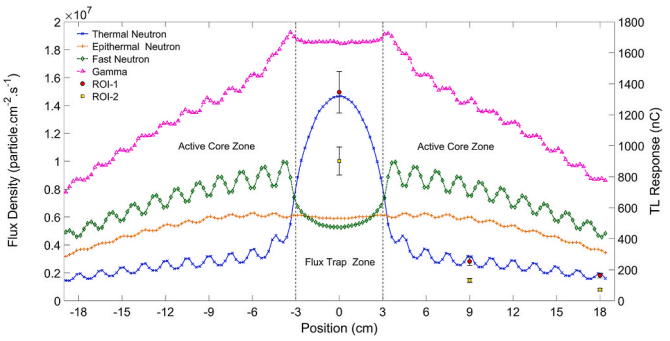

Fig. 4. TLD-100 responses and calculated photon and neutron fluxes profiles along the central channel (27.3 cm height) for the cylindrical core configuration.

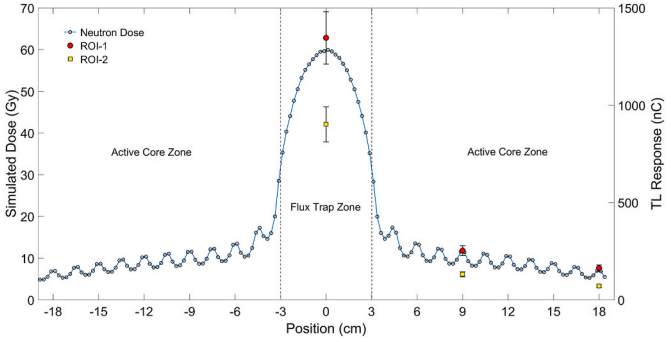

Fig. 5. TLD-100 responses and calculated thermal neutron dose delivered to it along the central channel (27.3 cm height) for the cylindrical core configuration.

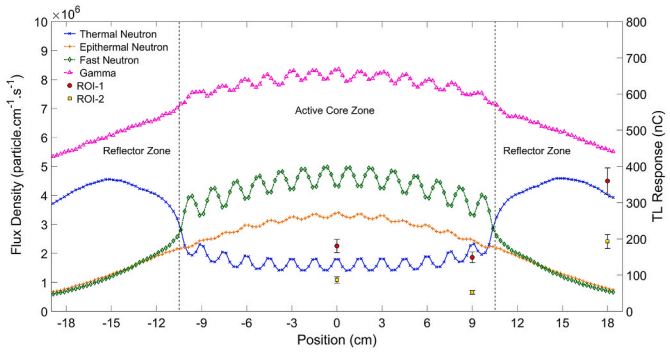

Fig. 6. TLD-100 responses and calculated photon and neutron fluxes profiles along the peripheral channel (27.3 cm height) for the cylindrical core configuration.

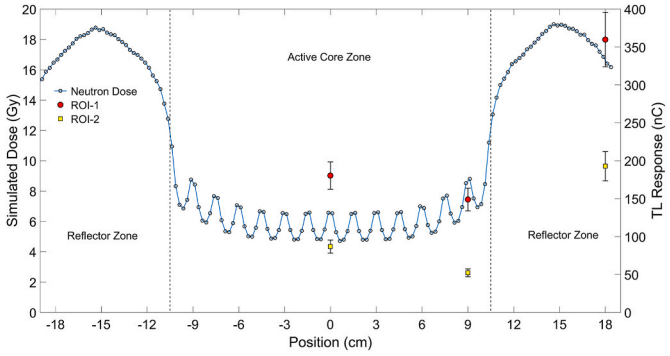

Fig. 7. TLD-100 responses and calculated thermal neutron dose delivered to it along the peripheral channel (27.3 cm height) for the cylindrical core configuration.

where the TLDs were placed as shown along Figs. 4–7, which correspond to half of the existed data for this core configuration, as data for the 45.6 cm quota were not show in these figures. The ratio values are relative to the adopted respective reference values found at the core central position (0 cm). Table 1 also presents the relative TL ratio responses for both ROIs.

Table 1 emphasizes the TLD response dependence with the thermal neutron flux and neutron dose, as it shows a comparison of dimensionless values. It corroborates the previous qualitative findings of an almost exclusively dependence of TLD-100 response with thermal neutron flux when this one is comparable to the gamma flux. Table 1 also highlights the good response/sensitivity to neutron field changes of TLD-100 ROI 1, standing as a superior TLD-100 response measure than ROI 2, which is usually considered a strict neutron sensitive TL region.

Considering the observed relationship between neutron dose and the TLD-100 ROI 1 response under many different mixed neutron gamma radiation fields, it was evident that a calibration curve relating these two parameters could be available. Fig. 8 shows the linear fit found and the 12 experimental data pairs obtained for the cylindrical configuration. Linear fit parameters are given by equation (4).

$$Dose_{neutron} = R.(23.8 \pm 1.2) + (40 \pm 20) \quad (4)$$

where $Dose_{neutron}$ is the calculated neutron dose (Gy) impinged onto TLD-100 and R is the TL-100 response given by its ROI 1 (nC).

As long as neutron and gamma field components are around the same order of magnitude, equation (4) relates the neutron dose delivered to TLD-100 with the TL response. This linear relationship is independent of how the neutron energy ranges are distributed or which field component prevails.

4.2. Experimental methodology evaluation

To verify the validity of using TLD-100 to investigate neutron dose within a research reactor, data extracted from 10 locations inside the rectangular core configuration were used to check if equation (4) is still valid for a different set of mixed neutron-gamma fields. Fig. 9 shows the correlation found between the simulated neutron dose deposited in the TLD 100 (eq. (3)) and the experimental methodology suggested in this work (eq. (4)). An identity reference line, i.e., a line drawn from points where y = x, is also presented in this figure. The average uncertainty on experimental neutron dose was set at 10%.

Analyzing the data of Fig. 9, it can be observed that the neutron dose obtained by the experimental methodology proposed in this work shows a good agreement with the values expected from simulations. For a better analysis of data compatibility, Fig. 10 presents the residual graph of this case.

The residual graph (Fig. 10) shows that all data are situated below 2 standard deviations, showing the good agreement between the simulated data and the data obtained via equation (4).

5. Conclusions

This work presented a dosimetric evaluation of the behavior of TLD-

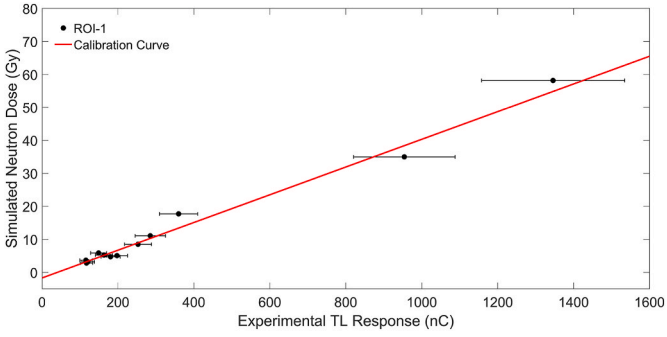

Fig. 8. TLD 100 ROI 1 calibration curve.

Table 1
Normalized values of calculated fluxes and doses in TLD-100 and measured ROIs responses in central and peripheral channels at height 27.3 cm in the cylindrical core configuration.

		Calculated Ratios					
		Simulated Values				Experimental Values	
Channel	Position [cm]	Thermal Neutron Flux	Gamma Flux	Neutron Dose	Gamma Dose	TLD-100 ROI 1	TLD-100 ROI 2
Central	0	1.000	1.000	1.000	1.000	1.000	1.000
Central	9	0.231 ± 0.002	0.771 ± 0.008	0.146 ± 0.006	0.905 ± 0.007	0.188 ± 0.027	0.146 ± 0.021
Central	18	0.141 ± 0.001	0.457 ± 0.004	0.090 ± 0.004	0.582 ± 0.004	0.121 ± 0.017	0.079 ± 0.011
Peripheral	0	0.120 ± 0.001	0.446 ± 0.003	0.081 ± 0.003	0.512 ± 0.006	0.134 ± 0.039	0.096 ± 0.014
Peripheral	9	0.152 ± 0.001	0.405 ± 0.003	0.101 ± 0.004	0.480 ± 0.005	0.111 ± 0.016	0.058 ± 0.008
Peripheral	18	0.271 ± 0.002	0.295 ± 0.002	0.305 ± 0.013	0.258 ± 0.003	0.267 ± 0.038	0.214 ± 0.030

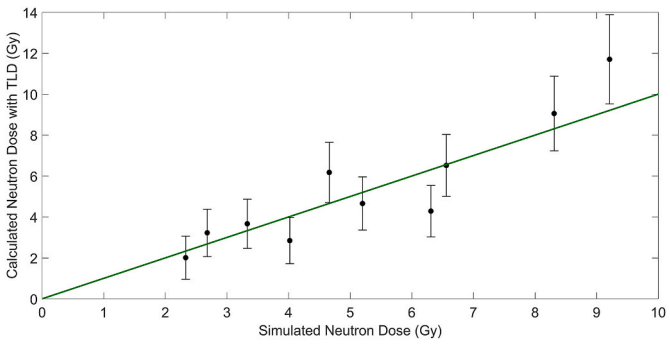

Fig. 9. Correlation between the deposited doses due to the neutrons in the TLD 100 calculated by the MCNP5 and the methodology created in this work.

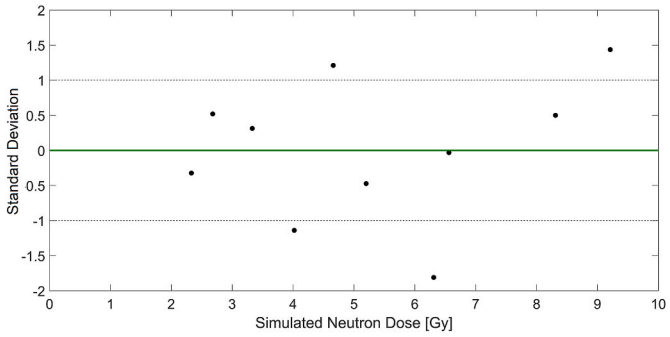

Fig. 10. Residual graph.

100 dosimeters exposed to a variety of mixed neutron-gamma fields. It showed that despite of the diversity of mixed radiation field characteristics, with different neutron energy spectra, neutron and gamma balance, and field intensity, a single dose response curve may be used. Such radiation field diversity was provided by the IPEN/MB-01 zero power research reactor installed at IPEN-CNEN. This versatile reactor is primarily used to perform benchmarked neutronic experiments; hence it presents very well defined construction parameters, which allow great confidence on estimating radiation field components via MCNP5 simulations. The quality of the data obtained showed that, besides being an excellent tool to perform neutronic experiments, the IPEN/MB-01 research reactor provides unique conditions to carry on dosimetric assessments.

Results have also shown that TLD-100 is particularly sensitive to thermal neutron and nearly insensitive to the gamma radiation field component at the irradiation conditions used, i.e. with radiation field component intensities around the same order of magnitude. This aspect has been even more evident for the TLD-100 ROI-1 than for TLD-100 ROI-2, the TL region usually linked to neutron interaction. These unexpected outcomes have been shown not only by the data presented in Table 1 but also by the linear correspondence found between neutron dose and TLD ROI-1 response.

It should be mentioned that TLD positioning in the core accounts for the most relevant experimental uncertainty source. On that account, the development of a more refined TLD positioning system in the core might be considered a possible step to drive more accurate results.

CRediT authorship contribution statement

Tássio Antonio Cavalieri: Conceptualization, Formal analysis, Investigation, Methodology, Writing – original draft, Writing – review & editing. **Paulo de Tarso Dalledone Siqueira:** Conceptualization, Formal analysis, Investigation, Methodology, Validation, Writing – original draft, Writing – review & editing. **Julian Marco Barbosa Shorto:** Conceptualization, Formal analysis, Investigation, Methodology, Writing – original draft, Writing – review & editing. **Helio Yoriyaz:** Formal analysis, Investigation, Methodology, Supervision, Validation, Writing – original draft, Writing – review & editing.

Declaration of competing interest

The authors declare the following financial interests/personal relationships which may be considered as potential competing interests: Tassio Antonio Cavalieri reports financial support was provided by Conselho Nacional de Desenvolvimento Científico e Tecnológico (CNPq).

Data availability

Data will be made available on request.

Acknowledgements

This work was partially supported by Conselho Nacional de Desenvolvimento Científico e Tecnológico (CNPq), Process number 142267/2014-7.

References

Bitelli, Ulysses d'Utra, Gonçalves, L.B., Kuramoto, R.Y.R., 2007. Calibration of nuclear power channels of the IPEN/MB-01 reactor: measurements of the spatial neutron flux distribution in the core using infinitely dilute gold foils. In: Proceedings of the INAC 2007 International Nuclear Atlantic Conference Nuclear Energy.

Bitelli, U.d'Utra, Martins, F.P.G., Jerez, R., 2009. Measurements of the neutron spectrum energy in the IPEN/MB-01 reactor core. Braz. J. Phys. 39, 39–43.

Carrillo, R.E., Uribe, R.M., Woodruff, G.L., Stoebe, T.G., 1987. Lithium fluoride (TLD-700) response to a mixed thermal neutron and gamma field. Radiat. Prot. Dosim. 19 (1), 55–57. https://doi.org/10.1093/oxfordjournals.rpd.a079920.

dos Santos, A., de Andrade e Silva, G.S., Fanaro, L.C.C.B., Yamagushi, M., Jerez, R., Diniz, R., Carneiro, A.L.G., Kuramoto, R.Y.R., Mendonça, A.G., Fuga, R., Maeda, R. M., Mura, L.F.L., 2012. IPEN (MB01)-LWR-CRIT-SPEC-REAC-COEF-KIN-RRATE-POWDIS-001:Reactor physics experiments in the IPEN/MB-01 research reactor facility. In: International Handbook of Evaluated Reactor Physics Benchmark Experiment. Paris:Nuclear Energy Agency (NEA DATA BANK), pp. 1–517.

dos Santos, A., Grant, C.R., Siqueira, P. de T.D., Tarazaga, A.E., de Andrade e Silva, G.S., Barberis, C.M., 2013. Validation of neutronic models and calculation systems by means of experimental results in the IPEN/MB-01 reactor. Ann. Nucl. Energy 60, 51–63. https://doi.org/10.1016/j.anucene.2013.04.022.

Ekendahl, D., Rubovic, P., Zlebcik, P., Huml, O., Mala, H., 2018. Dosimetry with salt in mixed radiation fields of photons and neutrons. Radiat. Protect. Dosim. 178, 329–332. https://doi.org/10.1093/rpd/ncx114.

Gambarini, G., Artuso, E., Giove, D., Felisi, M., Volpe, L., Barcaglioni, L., Agosteo, S., Garlati, L., Pola, A., Klupak, V., Viererbl, L., Vins, M., Marek, M., 2015a. Study of suitability of Fricke-gel-layer dosimeters for in-air measurements to characterise epithermal/thermal neutron beams for NCT. Appl. Radiat. Isot. 106, 145–150. https://doi.org/10.1016/j.apradiso.2015.07.036.

Gambarini, G., Artuso, E., Giove, D., Volpe, L., Agosteo, S., Barcaglioni, L., Campi, F., Garlati, L., Pola, A., Durisi, E., Borroni, M., Carrara, M., Klupak, V., Marek, M., Viererbl, L., Vins, M., D'Errico, F., 2015b. Fricke-gel dosimetry in epithermal or thermal neutron beams of a research reactor. Radiat. Phys. Chem. 116, 21–27. https://doi.org/10.1016/j.radphyschem.2015.03.025.

Gonçalves, L.B., 2008. Calibração dos Canais Nucleares do Reator IPEN/MB-01, Obtida a Partir da Medida da Distribuição Espacial do Fluxo de Nêutrons Térmicos no Núcleo do Reator Através da Irradiação de Folhas de Ouro Infinitamente Diluídas. IPEN.

Hakimi, A., Sohrabi, M., 2017. Photoneutron depth dose equivalent distributions in high-energy X-ray medical accelerators by a novel position-sensitive dosimeter. Phys. Med.-Eur. J. Med. Phys. 36, 73–80. https://doi.org/10.1016/j.ejmp.2017.03.010.

Lee, C.-C., Lee, Y.-J., Chen, S.-K., Chiang, B.-H., Tung, C.-J., Chao, T.-C., 2015. MCNPX simulation of proton dose distributions in a water phantom. Biomed. J. 38, 414–420. https://doi.org/10.4103/2319-4170.167078.

National Institute of Standards and Technology, 2010. X-Ray Mass Attenuation Coefficients. http://physics.nist.gov/PhysRefData/XrayMassCoef/tab4.html.

Pradhan, A.S., 1981. Thermoluminescence dosimetry and its applications. Radiat. Protect. Dosim. 1, 153–167. https://doi.org/10.1093/oxfordjournals.rpd.a079971.

Shultis, J.K., Faw, R.E., 2011. An MCNP primer. https://www.mne.k-state.edu/~jks/MCNPprmr.pdf.

Torkzadeh, F., Manouchehri, F., 2006. Thermal neutron fluence measurement in a research reactor using thermoluminescence dosimeter TLD-600. J. Radiol. Prot. 26, 97–103. https://doi.org/10.1088/0952-4746/26/1/006.

Triolo, A., Brai, M., Marrale, M., Gennaro, G., Bartolotta, A., 2007. Study of the glow curves of TLD exposed to thermal neutrons. Radiat. Protect. Dosim. 126, 333–336. https://doi.org/10.1093/rpd/ncm069.

Tsai, W.-C., Huang, C.-K., Jiang, S.-H., 2018. QA measurement of gamma-ray dose and neutron activation using TLD-400 for BNCT beam. Appl. Radiat. Isot. 137, 73–79. https://doi.org/10.1016/j.apradiso.2018.03.010.

van der Marck, S.C., 2012. Benchmarking ENDF/B-VII.1, JENDL-4.0 and JEFF-3.1.1 with MCNP6. Nucl. Data Sheets 113, 2935–3005. https://doi.org/10.1016/j.nds.2012.11.003.

X-5 Monte Carlo Team, 2003. MCNP - A General N-Particle Transport Code. Version 5 Report No. LA-UR-03-1987.

Zoia, A., Jouanne, C., Sireta, P., Leconte, P., Braoudakis, G., Wong, L., 2017. Analysis of dynamic reactivity by Monte Carlo methods: the impact of nuclear data. Ann. Nucl. Energy 110, 11–24. https://doi.org/10.1016/j.anucene.2017.06.012.